Multimed Tools Appl (2018) 77:12057–12072
DOI 10.1007/s11042-017-4858-8

A new hybrid denoising model based on PDEs

Neda Mohamadi[1] · **Ali R. Soheili**[1] · **Faezeh Toutounian**[1]

Received: 9 June 2016 / Revised: 12 April 2017 / Accepted: 22 May 2017 /
Published online: 6 June 2017

Abstract In this paper, a novel denoising algorithm based on the denoising methods of partial differential equations is presented. The proposed algorithm is obtained by using a stochastic algorithm for combining two denoising methods based on partial differential equations. The model provides a new approach for solving the contradiction in the image restoration. The new hybrid model has more ability to restore the image in terms of peak signal to noise ratio, blind/referenceless image spatial quality evaluator and visual quality, compared with each of denoising methods separately used. Experimental results show that our approach is more efficient in image denoising than the used denoising methods.

Keywords Image denoising · Stochastic optimization algorithm · PDE-based model

1 Introduction

In recent years, with the rapid development of various types of digital equipment, image has become an important expression form for information. Digital images can be obtained through different sensors such as photographic cameras, medical scanners and weather satellites. Images generally are at risk of contamination by noise during the acquisition, transmission and compression processes. Thus, it is fundamental to suppress the noise while preserving important features of the image. The main purpose of image denoising approaches is to recover a digital image that has been spoiled by noise.

Over the last years, a variety of methods have been proposed to deal with the denoising problem [45, 47–49]. Some linear filtering methods [38, 39] have been suggested to remove Gaussian and uniform noise in images. Other commonly used linear filtering are Wiener filter [18] and Mean filter [23, 44]. Nonlinear image filters [11, 12] have emerged to improve the effectiveness of linear filters, where the median filter is the most used nonlinear filtering [42]. Various wavelet-based techniques have also been proposed for image denoising [17, 21, 34,

✉ Ali R. Soheili
soheili@um.ac.ir

[1] Department of applied mathematics, Faculty of Mathematical Sciences, Ferdowsi University of Mashhad, Mashhad, Iran

36]. The sparse representation has received a lot of attention from the image processing, resulting in the appearance of many practical approaches [1, 13, 15, 29]. Image denoising techniques based on partial differential equation and Computational Fluid Dynamics (CFD) have been developed, such as Total Variation (TV) methods [8, 14, 26, 37], level set methods [40], essentially non oscillatory schemes [9], and nonlinear diffusion algorithms [7, 22, 24, 31].

Recently, Partial Differential Equation (PDE) approaches of image denoising, such as linear and nonlinear diffusion algorithms have become important. The linear diffusion methods have been derived from the use of the Gaussian filter in multi-scale image analysis [20]. In order to eliminate the adverse effects of linear PDE-based techniques like blurring, the nonlinear PDE-based approaches have attracted a lot of attention in image denoising and enhancement. The most frequently applied nonlinear PDE denoising method is the diffusion scheme developed by Perona and Malik [33]. Since then, many different techniques have been devised accordingly [43]. The nonlinear PDE-based approaches are able to smooth the images while preserving the edges and also preventing the localization problems of linear filtering.

There are a variety of methods to achieve the nonlinear PDEs. In image processing, it is a common practice to obtain them from the variational problems. Minimizing the energy function is believed to be the essential basis of any variational PDE techniques [4, 10]. The model which is known as the TV, has been developed by Rudin, Osher and Fatemi, and is based on the minimization of the TV norm. Many PDE approaches improving this model have also appeared and perfectly studied in the recent years [10].

For image denoising purposes, several ways have been suggested that use Genetic Algorithm (GA) [19, 25, 41]. Stochastic optimization is a generic term for optimization heuristics which include such approaches as genetic algorithms and simulated annealing [16]. These techniques apply algorithms that mimic natural processes, such as selection and mutation in natural evolution, or metallurgical processes, such as the annealing of metals, to evolve solutions for difficult and large problems.

Partial differential equations have proven to be a useful tool in image denoising procedures. The main idea is to deform an image with a PDE and achieve the expected image as a solution to this equation. Since the noise is related to high frequencies, it is difficult to remove the noise while preserving the important features, such as edges. Recently, some denoising methods by combining different PDE-based models have been proposed [46]. They often perform more diffusion in the flat areas of the image and less diffusion in the edges of the image. Different PDE-based denoising models have various manners during the time. The combination of suitable PDE-based denoising models often yields images with higher quality. In order to obtain an image with higher quality than those obtained by two PDE-based models, a novel image denoising algorithm has been proposed by using stochastic optimization algorithm for combination purposes. The algorithm highlights the role of better model in each time step. The new method has more denoising ability in terms of Peak Signal to Noise Ratio (PSNR), Blind/Referenceless Image Spatial QUality Evaluator (BRISQUE) and visual quality, compared with the used PDE-based denoising models.

The rest of this paper is organized as the following: The PDE-based approaches are briefly described in Section 2. The proposed algorithm is described in Section 3. In Section 4, we present our experimental results that confirm the efficiency of proposed method and finally some concluding remarks are presented in Section 5.

2 PDE-based models

The use of PDE for image denoising has become a main research topic in the past few years and a large number of PDE-based methods have been proposed. The Isotropic Diffusion (ID) model, the Anisotropic Diffusion (AD) such as the Perona-Malik (PM) model, and the Total Variation (TV) model are good applications based on PDEs. In this section, we briefly describe these models and also the well-balanced anisotropic scheme [5], which can be used as the PDE-based methods in Sections 3 and 4.

ID model is a linear diffusion model which is usually used to smooth an image. This model allows us to remove the noise very well, but unfortunately will blur the edge of image during removing the noise. ID model [46] is described as follows:

$$\begin{cases} \dfrac{\partial u}{\partial t} = \nabla.(\nabla u) + \lambda(u_0 - u), \\ \dfrac{\partial u}{\partial n} = 0 \quad \text{on } \partial\Omega \times (0,T), \\ u(x,y,t)|_{t=0} = u_0(x,y) \quad \text{in } \Omega, \end{cases} \tag{1}$$

where $u(x, y, t)|_{t=0} = u_0(x, y)$ is the initial condition, $u(x, y, t)$ is the restored version of the initial degraded image $u_0(x, y)$, ∇ is gradient operator with respect to the spatial variables x , y,and Ω is an open bounded domain in $\mathbb{R}^2$.

In order to avoid the blurring and localization problems of linear diffusion filtering, Perona and Malik [33] proposed a nonlinear diffusion method based on the following equation

$$\frac{\partial u}{\partial t} = \nabla.\Big(g\Big(|\nabla u|\Big)\nabla u\Big). \tag{2}$$

In [33] the following two diffusion functions are considered

$$g_1(s) = \frac{1}{1 + \left(\frac{s}{k}\right)^2}, \quad g_2(s) = \exp\left(-\left(\frac{s}{k}\right)^2\right), \tag{3}$$

where $k > 0$ is the contrast parameter. The choice of the diffusion function g heavily influences the process of controlling the smoothing. This function is defined to satisfy $lim_{s\to 0} g(s) = 1$ and $lim_{s\to\infty} g(s) = 0$, so that the diffusion is high while the gradient is small and vice-versa. As a result, the diffusion is maximal within uniform regions and stops across edges.

Using g_1 as a diffusivity function, the Perona-Malik's model is equivalent to minimize

$$E(u) = \int_\Omega \frac{k^2}{2} \mathrm{In}\big(k^2 + |\nabla u|^2\big)\mathrm{dxdy}, \tag{4}$$

where $\Omega \in \mathbb{R}^2$ is the image domain.

The PM model appears to be an ill-posed problem. It means the existence and uniqueness of the solution of (2) cannot be guaranteed. So when the noise and edge have the same gradient, it cannot be applied for denoising. Therefore, the PM model can cause Gibbs-type artifacts.

A general model of the anisotropic diffusion equation which was first proposed by Perona and Malik can be expressed [3] as follows:

$$\begin{cases} \dfrac{\partial u}{\partial t} = \nabla.(g(|\nabla u|)\nabla u) + \lambda(u_0 - u), \\ \dfrac{\partial u}{\partial n} = 0 \quad \text{on } \partial\Omega \times (0,T), \\ u(x,y,t)|_{t=0} = u_0(x,y) \quad \text{in } \Omega, \end{cases} \tag{5}$$

where $u(x, y, t)|_{t=0} = u_0(x, y)$ is the initial condition and Ω is an open bounded domain in $\mathbb{R}^2$.

The diffusion–reaction Eq. (5) consists of the PM process with an additional term $\lambda(u_0 - u)$, which punishes deviations of u from u_0. This term can retain characteristics of the original image and reduce distortion.

The total variation model was proposed by Rudin et al. [37] for edge- preserving and noise removal. The authors have taken the energy function of the image as

$$E(u) = \iint_{\Omega} \left(|\nabla u| + \frac{\lambda}{2}(u_0 - u)^2 \right) dxdy. \tag{6}$$

The first term in this equation is a smoothing term, while the second term preserves the edges and details. The total variation model has a capacity of handling edges and removing noise in a given image [6]. The TV denoising model [2] can be written as follows:

$$\begin{cases} \dfrac{\partial u}{\partial t} = \nabla . \left(\dfrac{\nabla u}{|\nabla u|} \right) + \lambda(u_0 - u), \\ \dfrac{\partial u}{\partial n} = 0 \quad \text{on } \partial\Omega \times (0, T), \\ u(x, y, t)|_{t=0} = u_0(x, y) \quad \text{in } \Omega, \end{cases} \tag{7}$$

where $u(x, y, t)|_{t=0} = u_0(x, y)$ is the initial condition and Ω is an open bounded domain in $\mathbb{R}^2$.

The TV model is a successful approach to recover images with sharp edges. Nevertheless the TV model produces a block effect when being applied for the flat areas, thus the local details characteristics of the original image is lost [27, 28].

Anisotropic diffusion is a key concept in digital image denoising. In order to develop the idea of removing noise without losing the boundaries or edges, the authors in [5] have proposed an anisotropic nonlinear diffusion equation that has two terms: the diffusion and the forcing term. The balance between these terms has been made in a selective manner, in which boundary points and interior points of the objects that make up the image are treated differently. The following Well-Balanced Flow (WBF) equation has been considered

$$\begin{cases} \dfrac{\partial u}{\partial t} = g|\nabla \mathrm{u}|\nabla . \left(\dfrac{\nabla u}{|\nabla u|} \right) - \lambda(1 - g)(u - u_0), \quad x \in \Omega, t > 0 \\ \dfrac{\partial u}{\partial n} = 0 \quad x \in \partial\Omega \quad , t > 0 \\ u(x, y, t)|_{t=0} = u_0(x, y) \quad \text{in } \Omega \end{cases} \tag{8}$$

where $g = g(|G_\sigma * \nabla u|)$, $u_0(x, y)$ is an image to be processed, $u(x, y, t)$ represents its smoothed version in the scale t, G_σ is a convolution kernel (here, a Gaussian function), and $G_\sigma * \nabla u$ is the local estimate of ∇u used for noise elimination. The function $g(s) \geq 0$ is a nonincreasing function, satisfying $g(0) = 1$ and $g(s) \to 0$ when $s \to \infty$.

3 New model

From the fact that minimizing the combination of suitable denoising energy functions (or combination PDE-based models) often yields images with higher quality, a hybrid model with random weight has been presented, which highlights the role of better model in each time step. In addition, a stochastic algorithm for being able to use any two PDE-based models (not fixed models with perfect information) has been employed. The method gradually evolves a population of solutions with the goal in mind of steadily improving the best solution.

Here we assumed that a solution (individual) is a matrix of pixels, whose entries are integer values ranging the interval [0, 255]. Before describing the stages of the algorithm in detail, we introduce some notations for our discussion. u_0 denotes the input noisy image. We denote by M_i a PDE-based denoising model, such as ID, PM, TV, WBF or any other suitable PDE-based model. For simplicity, we assume that $i = 1, 2$. $u_{M_i}^k$ denotes the solution of M_i model on the

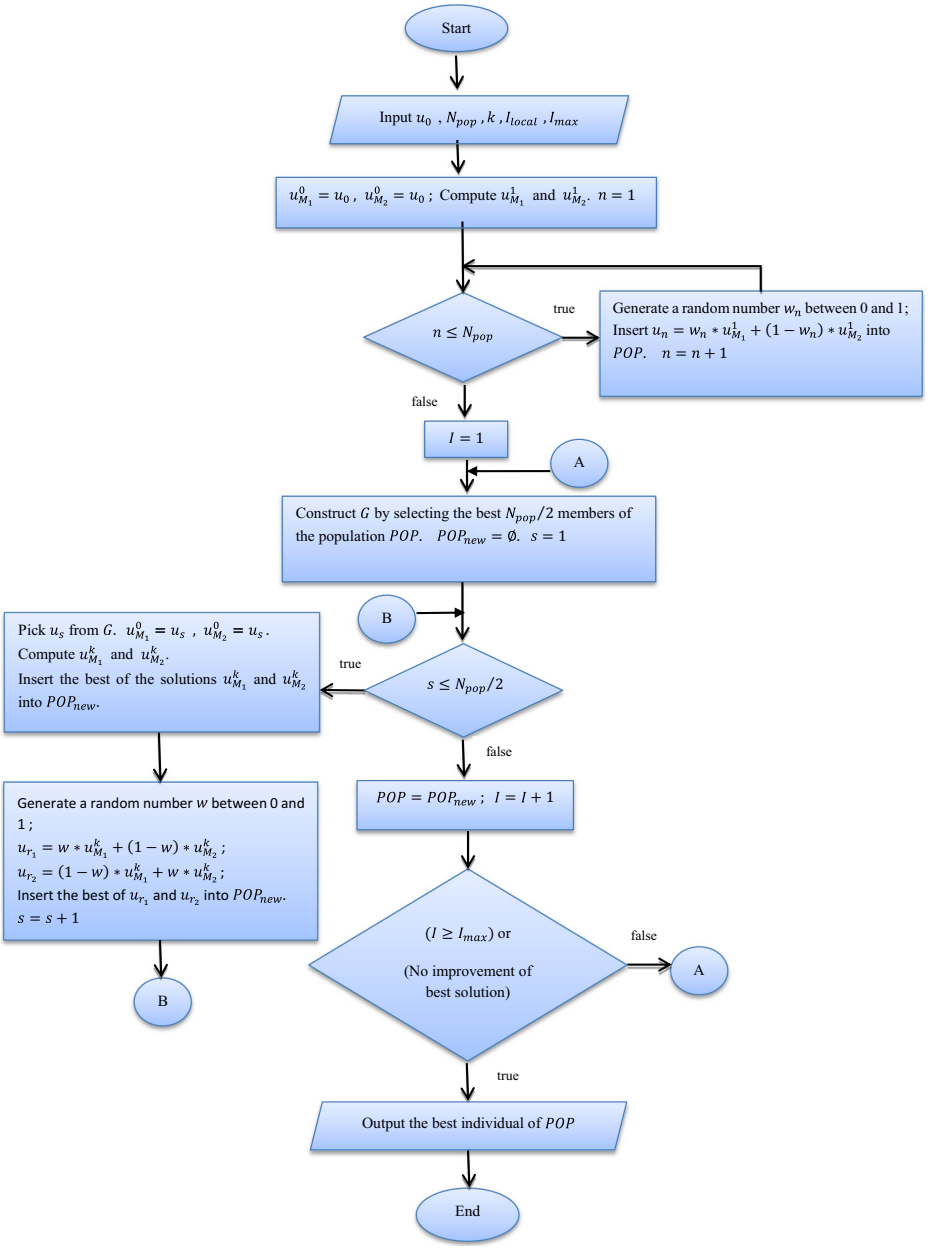

Fig. 1 Flow diagram

time level k. For small k ($k = 1, 2, 3$), we consider $u^k_{M_i}$ as a neighbor of the solution $u^0_{M_i}$ which is an initial solution for M_i model.

The algorithm (whose processing steps are presented in Fig. 1) starts by generating some solutions randomly, evaluating them and inserting them into the population. For constructing a new population, a population generator is produced by selecting one half the individuals of current population which have the highest fitness values. The individuals of a new population are derived from the existing solutions in the population generator in two ways. In the first, two solutions in the neighborhood of existing solution are generated and evaluated, then the best solution is inserted into the new population. The second way generates a new solution randomly, as was done during initialization. The purpose of generating a solution randomly is to introduce new solutions, possibly different from those exist in the population, in order to prevent the population from converging prematurely [32]. After the construction of the new population is completed, its best solution will be considered as the best current solution. Finally, the algorithm terminates when no improvement has taken place in the best current solution for a pre-determined number of iterations or a predefined maximum number of iterations is achieved.

In detail the new algorithm has five stages:

1- Initialization
2- Evaluation
3- Selection
4- Solution generation
5- Termination

3.1 Initialization

The algorithm starts by constructing a group of individuals (images) known as the initial population. The population will have N_{pop} individuals (N_{pop}will provide by the user, for

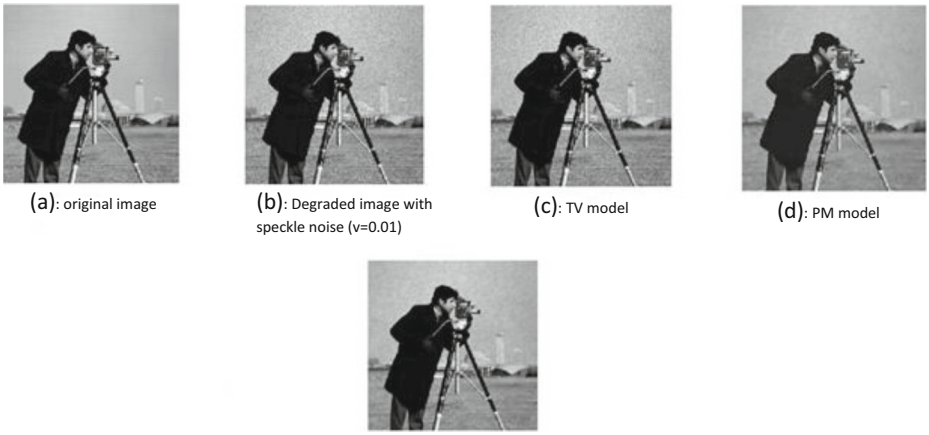

Fig. 2 Denoising results of the 15th iteration of the denoising models

Table 1 The PSNRs and BRISQUEs of the 15th iteration ($\Delta t = 0.1$) of the PM, TV, and the new model (hybrid of TV and PM). Input Cameraman image is corrupted by speckle noise of variance 0.01

Model	PM model	TV model	New model
PSNR	29.1799	27.0463	30.2427
BRISQUE	49.2757	49.7596	29.8186

example $N_{pop} = 30$). By taking $u^0_{M_1} = u_0$ and $u^0_{M_2} = u_0$, the individuals of initial population will be defined as follows:

$$u_n = w_n * u^1_{M_1} + (1 - w_n) * u^1_{M_2}, \quad n = 1, 2, \ldots, N_{pop}, \tag{9}$$

where w_n is a random number between 0 and 1.

3.2 Evaluation

In order to determine the qualities of the individuals in a population, the fitness values are computed by using the No-Reference image quality assessment model BRISQUE (http://live.ece.utexas.edu/research/quality/BRISQUE_release.zip). This evaluator uses scene statistics of locally normalized luminance coefficients to quantify possible losses of naturalness in the image, due to the presence of distortion and the BRISQUE can be considered as a holistic measure of quality.

3.3 Selection

In order to improve the current best solution, in each iteration, we construct a generator as follows: First, the fitness values and associated individuals are ranked from highest fitness value to lowest fitness value. Then, the best $N_{pop}/2$ members of the population are selected for constructing the generator G. From the fact that evaluator BRISQUE is a holistic measure of quality [30], this step of algorithm tries to discard the images with low quality in the new population.

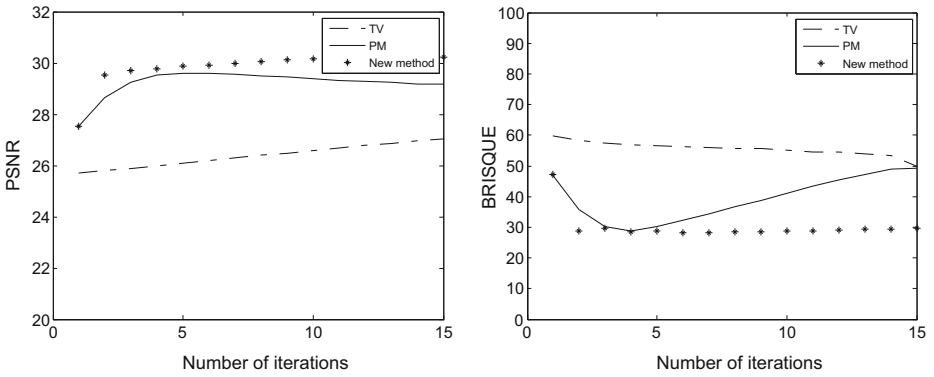

Fig. 3 The PSNR and BRISQUE graphs of the TV model, PM model, and new model (hybrid of TV and PM) for various number of iterations ($\Delta t = 0.1$). Input Cameraman image is corrupted by speckle noise of variance 0.01

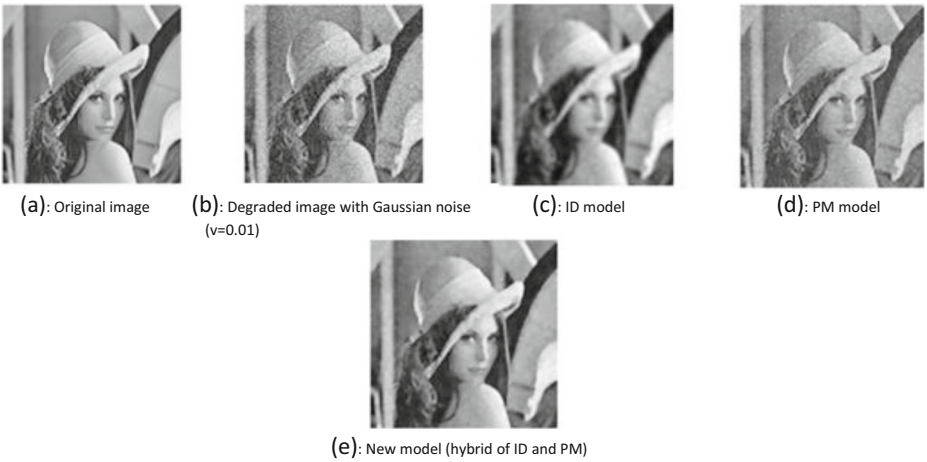

Fig. 4 Denoising results of the 30th iteration of the denoising models

3.4 Solution generation

By considering each $u_s \in G$ as an initial condition for PDEs models (i. e., $u^0_{M_1} = u_s$ and $u^0_{M_2} = u_s$), two individuals will be generated for the new population, by the following ways:

1- The first way computes the solutions $u^k_{M_1}$ and $u^k_{M_2}$ (the neighbors of u_s), by using the denoising models M_1 and M_2, respectively. Then, the new individual u_{new1} for the new population is obtained by choosing the best solution between $u^k_{M_1}$ and $u^k_{M_2}$, according to the Fitness function.

2- The second way generates a new individual u_{new2} which is defined as the best solution between:

$$w * u^k_{M_1} + (1-w) * u^k_{M_2} \quad \text{and} \quad (1-w) * u^k_{M_1} + w * u^k_{M_2},$$

where w is a random number between 0 and 1. By using the weight w and $(1 - w)$ and selecting the best solution, the image generated by the model with higher quality (in terms of BRISQUE) has more influence in constructing the new image.

3.5 Termination

Under these two conditions the process terminates:

(i) No improvement has taken place in the best solution for a pre-determined number of iterations,
(ii) A predefined maximum number of iterations is achieved.

Table 2 The PSNRs and BRISQUEs of the 30th iteration ($\Delta t = 0.1$) of the ID, PM, and new model (hybrid of ID and PM). Input Lena image is corrupted by Gaussian noise of variance 0.01

Model	ID model	PM model	New model
PSNR	24.4115	24.8722	28.2009
BRISQUE	64.3422	75.1499	24.4196

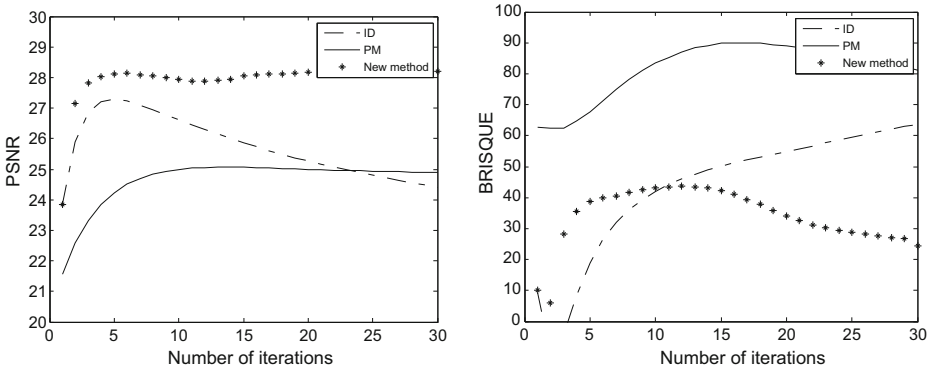

Fig. 5 The PSNR and BRISQUE graph of the ID model, PM model, and the new model (hybrid of ID and PM) for various number of iterations ($\Delta t = 0.1$). Input Lena image is corrupted by Gaussian noise of variance 0.01

The processing steps of the algorithm are presented in Fig. 1.

4 Experimental results and analysis

For the experimental results, the ID, PM, TV, and WBF models were used as the PDE-based models. In this section, we compare the experimental results obtained by the new method with the results obtained by the used PDE-based denoising models in terms of the visual quality of denoising image, PSNR according to (10), and Blind/Referenceless Image Spatial QUality Evaluator BRISQUE as described in Section 3.2. The PSNR is defined in decibels for 8-bit gray-scale images, as follows:

$$PSNR = 10log\frac{255^2 \times M \times N}{\sum_{i=1}^{M}\sum_{j=1}^{N}[I_{\mathrm{or}}(i,j) - I_{de}(i,j)]^2}, \tag{10}$$

where M and N are the image dimensions, I_{or} is the original image, I_{de} is the denoised image, and 255 is the peak signal with an 8-bit resolution. A higher PSNR usually indicates that the image is of higher quality. The BRISQUE is a No-Reference image quality assessment model, which determines the quality score of the image and the score typically has a value between 0 and 100 (0 represents the best quality, 100 the worst).

The proposed method with the parameters $N_{pop} = 30$, $I_{max} = 50$, $I_{local} = 5$, $k = 3$, has been tested on several images; some of them are selected to illustrate the results. The commonly used 256×256 bit Cameraman, Lena, and House images are taken in figures.

Table 3 The PSNR of the 30th iteration($\Delta t = 0.1$) of different algorithms with different variances of Gaussian noise

Variance of the noise	0.01	0.02	0.03
ID model	24.4115	24.1903	23.9166
PM model	24.8722	20.1237	17.6511
New model (hybrid of ID and PM)	28.2009	26.7897	25.6011

Table 4 The BRISQUE of the 30th iteration ($\Delta t = 0.1$) of different algorithms with different variances of Gaussian noise

Variance of the noise	0.01	0.02	0.03
ID model	64.3422	62.1667	62.2467
PM model	75.1499	95.0237	92.4674
New model (hybrid of ID and PM)	24.4196	30.5439	31.4609

In Fig. 2, we present the original Cameraman image, the corrupted image by speckle noise of variance 0.01, the results obtained by the TV model, the PM model, and our new model (hybrid of TV and PM). Table 1 contains the PSNRs and BRISQUEs of the PM, TV, and the new models. Figure 3 shows the PSNR and BRISQUE graphs of these models and indicates that the new model has higher PSNR and lower BRISQUE than the TV and PM models.

In Fig. 4, we present the original Lena image, the corrupted image by Gaussian noise of variance 0.01, the results obtained by the ID model, PM model, and the new model (hybrid of ID and PM). The PSNRs and the BRISQUEs of the ID model, PM model, and the new model are shown in Table 2. In Fig.5, we have plotted the PSNR and BRISQUE of these models. It can be seen that the PSNR of the new method has higher PSNR of the other models and after a few iterations the BRISQUE of the hybrid model becomes lower than the BRISQUE of the ID and PM models.

Tables 3 and 4 present the PSNR and BRISQUE, respectively, for different variances of the Gaussian noise. As expected, the new method has the highest PSNR and the lowest BRISQUE for different variances of the noise.

Figure 6 demonstrates the original House image, the corrupted image by Gaussian noise of variance 0.01, the results obtained by the WBF model, PM model, and the new model (hybrid of WBF and PM). Table 5 Contains the PSNRs and BRISQUEs of the WBF model, PM model, and the new model. Figure 7 shows the PSNR and BRISQUE

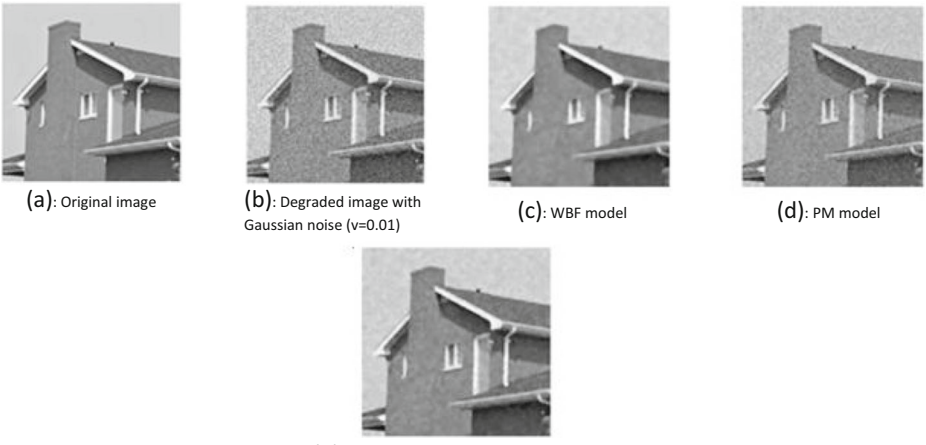

Fig. 6 Denoising results of the 8th iteration of the denoising models

Table 5 The PSNR and BRISQUE of the 8th iteration($\Delta t = 0.4$) of the WBF, PM, and new model (hybrid of WBF and PM). Input House image is corrupted by Gaussian noise of variance 0.01

Model	WBF model	PM model	New model
PSNR	29.7771	26.1440	30.0348
BRISQUE	55.3304	90.0515	44.7899

graphs of these models. It can be seen that the results are similar to those of the Cameraman and the Lena images.

For comparing the new model with different diffusion based schemes presented in [35], we used, as the noisy images, the images obtained by adding Gaussian noise of strength $\sigma_n = 25$ to the original Lena and the original House images. Table 6 shows the PSNR of some diffusion schemes presented in [35] and the new model for Lena and House images. These diffusion schemes are Anisotropic Diffusion (AD), Smoothed Gradient based anisotropic diffusion (SG), Total Variation (TV), Mean Curvature Motion (MCM), Well- Balanced Flow (WBF), Modified Smoothed Gradient (MSG) based anisotropic diffusion, Edge Enhancing Diffusion (EED), Coherence Enhancing Diffusion (CED), Slowed Anisotropic Diffusion (SAD), Adaptive TV (ATV), Adaptive Linear Diffusion (ALD), Edge detector based Anisotropic Diffusion (EAD), Weighted Linear Diffusion (WLD) and Weighted and Well- Balanced Flow (WWBF). It can be seen that the new model performs better than the most or on a par with a few other methods.

So, from the experimental results, we can conclude that the new method is an efficient model in image denoising.

5 Conclusion

We proposed a new approach for image denoising by introducing a stochastic optimization algorithm for combining PDE-based denoising methods such as the ID

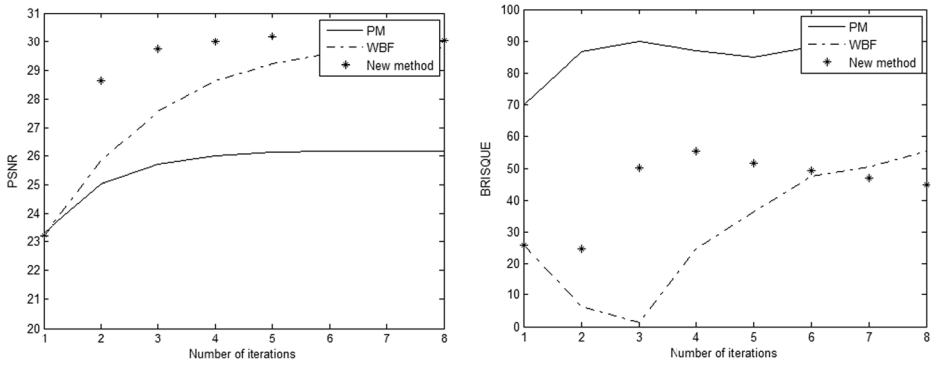

Fig. 7 The PSNR and BRISQUE graphs of the PM model, WBF model, and the new model (hybrid of PM and WBF) for various number of iterations ($\Delta t = 0.4$). Input House image is corrupted by Gaussian noise of variance 0.01

Table 6 PSNR comparison for different diffusion based schemes. Noisy images are obtained by adding Gaussian noise of strength $\sigma_n = 25$ to the original Lena and House images

Scheme	AD(PM)	SG	TV	MCM	WBF	MSG	EED	CED	SAD	ATV	ALD	EAD	WLD	WWBF	New model
Lena	26.32	23.26	27.05	23.97	26.46	26.53	27.23	23.97	25.85	27.26	20.70	24.88	23.87	27.12	**28.24**
House	28.87	24.94	30.18	25.89	28.94	29.30	30.68	25.89	29.18	30.39	23.23	28.17	27.03	30.92	**30.20**

model, the PM model, the TV model, and the WBF model. The new denoising model provides a new approach which is more efficient in image denoising than the used PDE- based denoising methods. To illustrate the superiority of the proposed model, we have used the Peak Signal to Noise Ratio (PSNR) and Blind/Referenceless Image Spatial QUality Evaluator (BRISQUE) as the subjective criterion. Numerical experiments show that our algorithm has higher PSNR and lower BRISQUE than the used denoising methods. Our experimental results confirm the high performance of the proposed model.

Acknowledgements The authors are grateful to three anonymous referees for their valuable comments which substantially improved the quality of this paper.

References

1. Aharon M, Elad M, Bruckstein A (2006) The K-SVD: an algorithm for designing of overcomplete dictionaries for sparse representation. IEEE Trans Image Process 54(11):4311–4322
2. Andreu F, Mazón JM, Moll JS (2005) The total variation flow with nonlinear boundary conditions. Asymptot Anal 43(1–2):9–46
3. Aubert G, Kornprobst P (2006) Mathematical problems in image processing PDEs and the calculus of variations, 2nd edn. Springer, New York
4. Barbu T, Barbu V, Biga V, Coca D (2009) A PDE variational approach to image denoising and restorations. Nonlinear Anal RWA 10:1351–1361
5. Barcelos CAZ, Boaventura M, Silva EC Jr (2003) A well-balanced flow equation for noise removal and edge detection. IEEE Trans Image Process 12(7):751–763
6. Beck A, Teboulle M (2009) Fast gradient-based algorithms for constrained total variation image denoising and deblurring problems. IEEE Trans Image Process 18(11):2419–2434
7. Black MJ, Sapiro G, Marimont DH, Heeger D (1998) Robust anisotropic diffusion. IEEE Trans Image Process 7(3):421–432
8. Chambolle A (2004) An algorithm for total variation minimization and applications. J Math Imaging Vision 20(1–2):89–97
9. Chan T, Zhou H (1999) Adaptive ENO-wavelet Transforms for Discontinuous Functions. Computational and Applied Mathematics Technical Report, Department of Mathematics, UCLA. Tech. Rep. 99–21, Jun. 1999
10. Chan T, Shen J, Vese L (2003) Variational PDE models in image processing. Notices of the AMS 50(1):14–26
11. Chaux C, Duval L, Benazza-Benyahia A, Pesquet JC (2008) A nonlinear stein-based estimator for multichannel image denoising. IEEE Trans Signal Process 56(8):3855–3870
12. Chen B, Li Y, Cai JL (2012) Noisy image segmentation based on nonlinear diffusion equation model. Appl Math Model 36(3):1197–1208
13. Dong W, Li X, Zhang L, Shi G (2011) Sparsity-based image denoising via dictionary learning and structural clustering. CVPR 2011 (oral)
14. Drapaca C (2009) A nonlinear total variation-based denoising method with two regularization parameters. IEEE Trans Biomed Eng 56(3):582–586
15. Elad M, Aharon M (2006) Image denoising via sparse and redundant representations over learned dictionaries. IEEE Trans Image Process 15(12):3736–3745
16. Fouskakis D, Draper D (2002) Stochastic optimization: a review. Int Stat Rev 70(3):315–349
17. Gai S, Luo L (2015) Image denoising using normal inverse Gaussian model in quaternion wavelet domain. Multimedia Tools and Applications 74(3):1107–1124
18. Gonzalez RC, Woods RE (2006) Digital Image Processing. Prentice-Hall, Inc., Upper Saddle River
19. Isgrò F, Tegolo D (2008) A distributed genetic algorithm for restoration of vertical line scratches. Parallel Comput 34(12):727–734
20. Jain AK (1989) Fundamentals of digital image processing. Prentice Hall, NJ
21. Jain P, Tyagi V (2017) An adaptive edge-perserving image denoising technique using patch-based weighted_ SVD filtering in wavelet domain. Multimedia Tools and Applications 76(2):1659–1679

22. Jin JS, Wang Y, Hiller J (2000) An adaptive nonlinear diffusion algorithm for filtering medical images. IEEE Trans Inf Technol Biomed 4(4):298–305
23. Kaisar S, Rijwan S, Al Mahmud J, Rahman MM (2008) Salt and pepper noise detection and removal by tolerance based selective arithmetic Mean filtering technique for image restoration. International Journal of Computer Science and Network Security 8(6):271–278
24. Katkovnik V, Egiazarian AJ (2006) Local approximation techniques in signal and image processing. SPIE Press. Monograph, vol PM157
25. Korürek M, Yüksel A, Iscan Z, Dokur Z, Ölmez T (2010) Retr-ospective correction of near field effect of X-ray source in radiographic images by using genetic algorithms. Expert Syst Appl 37(3): 1946–1954
26. Kumar M, Dass S (2009) A total variation-based algorithm for pixel-level image function. IEEE Trans Image Process 18(9):2137–2143
27. Lysaker M, Lundervold A, Tai X-C (2003) Noise removal using fourth-order partial differential equation with application to medical magnetic resonance images in space and time. IEEE Trans Image Process 12(12):1579–1590
28. Lysaker M, Osher S, Tai X-C (2004) Noise removal using smoothed normal and surface fitting. IEEE Trans Image Process 13(10):1345–1357
29. Mairal J, Elad M, Sapiro G (2008) Sparse representation for color image restoration. IEEE Trans Image Process 17(1):53–69
30. Mittal A, Moorthy AK, Bovik AC (2012) No-reference image quality assessment in the spatial domain. IEEE Trans Image Process 21(12):4695–4708
31. Monteil J, Beghdadi A (1998) A new adaptive nonlinear anisotropic diffusion for noise smoothing. In: IEEE International conference on image processing, vol. 3. Chicago Oct 1998, pp 254–258
32. Pargas RP, Jain R (1993) A parallel algorithm for solving 2D bin packing problems. In: ICNN, pp 18–25
33. Perona P, Malik J (1987) Scale space and edge detection using anisotropic diffusion. In: Proc. of IEEE Computer society workshop on Computer Vision, pp. 16–22 (November 1987)
34. Portilla J, Strela V, Wainwright MJ, Simoncelli EP (2013) Image denoising using scale mixtures of gaussians in the wavelet domain. IEEE Trans Image Process 12(11):1338–1351
35. Prasath VBS, Vorotnikov D (2014) Weighted and well-balanced anisotropic diffusion scheme for image denoising and restoration. Nonlinear Anal Real World Appl 17:33–46
36. Ram I, Elad M, Cohen I (2011) Generalized tree-based wavelet transform. IEEE Trans Signal Process 59(9): 4199–4209
37. Rudin L, Osher S, Fatemi E (1992) Nonlinear total variation based noise removal algorithms. Phisica D: Nonlinear Phenomena 60(1):259–268
38. Russo F (2003) A method for estimation and filtering of Gaussian noise in images. IEEE Trans Instrum Meas 52(4):1148–1154
39. Russo F (2004) Image filtering based on piecewise linear models. In: IEEE International Workshop IST, Stresa, Italy, May 2004, pp 7–12
40. Sethian JA (1999) Level set methods and fast marching methods: evolving interfaces in Computational geometry, fluid mechanics, Computer Vision and Materials Sciences. Cambridge University Press
41. Toledo CFM, de Oliveira L, da Silva RD, Pedrini H (2013) Image denoising based on genetic algorithm. In IEEE Congress on Evolutionary Computation, pp. 1294–1301
42. Tukey JW (1974) Nonlinear methods for smoothing data. In: Conf. Rec. EASCON`74, 1974, pp 673
43. Weickert J (1998) Anisotropic diffusion in image processing. European consortium for mathematics in industry. B. G. Teubner, Stuttgart
44. Windyga PS (2001) Fast impulsive noise removal. IEEE Trans Image Process 10(1):173–178
45. Xu P, Miao Q, Tang X, Zhang J (2014) A denoising algorithm via wiener filtering in the shearlet domain. Multimedia Tools and Applications 71(3):1529–1558
46. Yahya AA, Tan JQ, Hu M (2014) A blending method based on partial differential equations for image denoising. Multimedia Tools and Applications 73(3):1843–1862
47. Yin X, Zhou S, Abubakar M (2016) Fractional nonlinear anisotropic diffusion with P-Laplace variation method for image restoration. Multimedia Tools and Applications 75(8):4505–4526

48. Zeng W, Lu X, Tan X (2015) A local structural adaptive partial differential equation for image denoising. Multimedia Tools and Applications 74(3):743–757
49. Zhang X, Feng X (2015) Image denoising using local adaptive wiener filter in the gradient domain. Multimedia Tools and Applications 74(23):10495–10514

Neda Mohamadi is a Ph.d. student in Numerical analysis at department of applied mathematics of Ferdowsi University of Mashhad (FUM), Mashhad, Iran. She received her M.Sc. degree in Applied Mathematics from FUM in 2002. She has worked as an academic member at Shirvan branch of the Islamic azad university (IAU) during 2003–2011 and moved to Mashhad branch of IAU since 2012. Her research interest include Image processing and Genetic algorithms.

Ali R. Soheili serves as a Professor in applied mathematics at the Ferdowsi University of Mashhad, Iran. He has been working on numerical solution of ordinary, partial and stochastic differential equations using discretization, adaptive time-stepping, and meshless methods. One of his researches focuses on PDE variational approaches to image denoising and restoration.

Faezeh Toutounian received the B.S. degree in mathematics from Ferdowsi University of Mashhad (Iran) and the M.S. degree and the Ph.D. degree in applied mathematics from Pierre and Marie Curie University of Paris (France) in 1970, 1971, and 1975, respectively. She is currently a professor with the Department of Applied Mathematics, Ferdowsi University of Mashhad. Her research interests include numerical linear algebra, iterative methods in numerical linear algebra, and mathematical methods in image processing.